Synthetic and Systems Biotechnology 5 (2020) 121–130

Contents lists available at ScienceDirect

Synthetic and Systems Biotechnology

journal homepage: http://www.keaipublishing.com/synbio

Metabolic engineering of a methyltransferase for production of drug precursors demecycline and demeclocycline in *Streptomyces aureofaciens*

Weinan Yang, Lingxin Kong, Qing Wang, Zixin Deng, Delin You*

State Key Laboratory of Microbial Metabolism, Joint International Research Laboratory of Metabolic and Developmental Sciences, School of Life Sciences & Biotechnology, Shanghai Jiao Tong University, Shanghai, 200030, China

ARTICLE INFO

Keywords:
Demecycline
Demeclocycline
Streptomyces aureofaciens F3
Metabolic engineering

ABSTRACT

Demecycline (DMTC) and demeclocycline (DMCTC) are C6-demethylated derivatives of tetracycline (TC) and chlortetracycline (CTC), respectively. They are precursors of minocycline and tigecycline, which showed remarkable bioactivity against TC-resistant bacteria and have been used clinically for decades. In order to biosynthesize drug precursors DMTC and DMCTC, the function of a possible C-methyltransferase encoding gene *ctcK* was studied systematically in the CTC high-yielding industrial strain *Streptomyces aureofaciens* F3. The *ΔctcK* mutant accumulated two new products, which were turned out to be DMTC and DMCTC. Meanwhile, time-course analysis of the fermentation products detected the epimers of DMTC and DMCTC transformed spontaneously. Finally, an engineering strain with higher productivity of DMCTC was constructed by deleting *ctcK* and overexpressing *ctcP* of three extra copies simultaneously. Construction of these two engineering strains not only served as a successful example of synthesizing required products through metabolic engineering, but also provided original strains for following elaborate engineering to synthesize more effective tetracycline derivatives.

1. Introduction

Tetracyclines (TCs) are characterized by the tetracyclic naphthacene core and could inhibit protein synthesis by binding the 30S ribosomal subunit [1,2]. Tolerance of chemical modifications on ring C and ring D in TC contributed to the successful synthesis of the second and third generations of TCs with enhanced antibiotic activity and pharmacological properties, such as doxycycline, minocycline, tigecycline and omadacycline [1]. Minocycline (7-dimethylamino-6-dimethyl-6-deoxytetracycline) (Fig. 1A) is one of the second-generation TCs, and possesses attractive advantages such as better absorption, longer half-life and almost complete bioavailability [3–6]. It is used for the treatment of acne vulgaris and some sexually transmitted diseases, and it also exhibits multiple non-antibiotic activities including anti-inflamation, anti-autoimmune disorders and neuroprotection [7–9]. Tigecycline (9-*t*-butylglycylamido-minocycline) (Fig. 1A) is the first glycylcycline derived from minocycline, and it was also referred to as one of the third-generation TCs [10]. It can overcome most of the currently known tetracycline resistance mechanisms, especially efflux pumps and ribosomal protection [11,12]. Thus, it showed notable activity against methicillin-resistant *Staphylococcus aureus* (MRSA), vancomycin-resistant enterococci (VRE), and penicillin-resistant *Streptococcus pneumonia* (PRSP) [13]. Because of its prominent antibacterial effect, tigecycline was approved by FDA for the treatment of complicated skin and skin structure infections (cSSSIs) as well as complicated intra-abdominal infections (cIAIs) in 2005 [14,15].

Demecycline (DMTC) and demeclocycline (DMCTC) (Fig. 1B) can be reduced to sancycline (6-demethyl-6-deoxytetracycline), the minimum structure necessary for antimicrobial activity, and then converted to 7-aminosancycline or minocycline [4,16]. The achievable transformation from DMTC and DMCTC to minocycline and tigecycline made them important drug precursors. Total chemical synthesis of DMTC and DMCTC is a time-consuming and high-cost process [17], so high-efficient biosynthesis is still required, which in turn calls for detailed illustration on the biosynthesis machinery. To date, TCs such as chlortetracycline (CTC) [18], tetracycline (TC) [19] (Fig. 1B) and oxytetracycline (OTC) [20] have been found to be produced by many *Streptomyces*. Moreover, microbial productivities of natural TCs have been dramatically improved, benefiting from random mutagenesis in combination with optimization of fermentation conditions [21,22], metabolic engineering approaches [23–25] and genetic manipulation of regulatory genes [26,27]. All these efforts set important stage for engineering construction of DMTC and DMCTC high-yielding strains. In fact, during the study of the CTC-producing strain *S. aureofaciens*,

Peer review under responsibility of KeAi Communications Co., Ltd.
* Corresponding author.
E-mail address: dlyou@sjtu.edu.cn (D. You).

https://doi.org/10.1016/j.synbio.2020.06.001
Received 25 February 2020; Received in revised form 2 June 2020; Accepted 3 June 2020

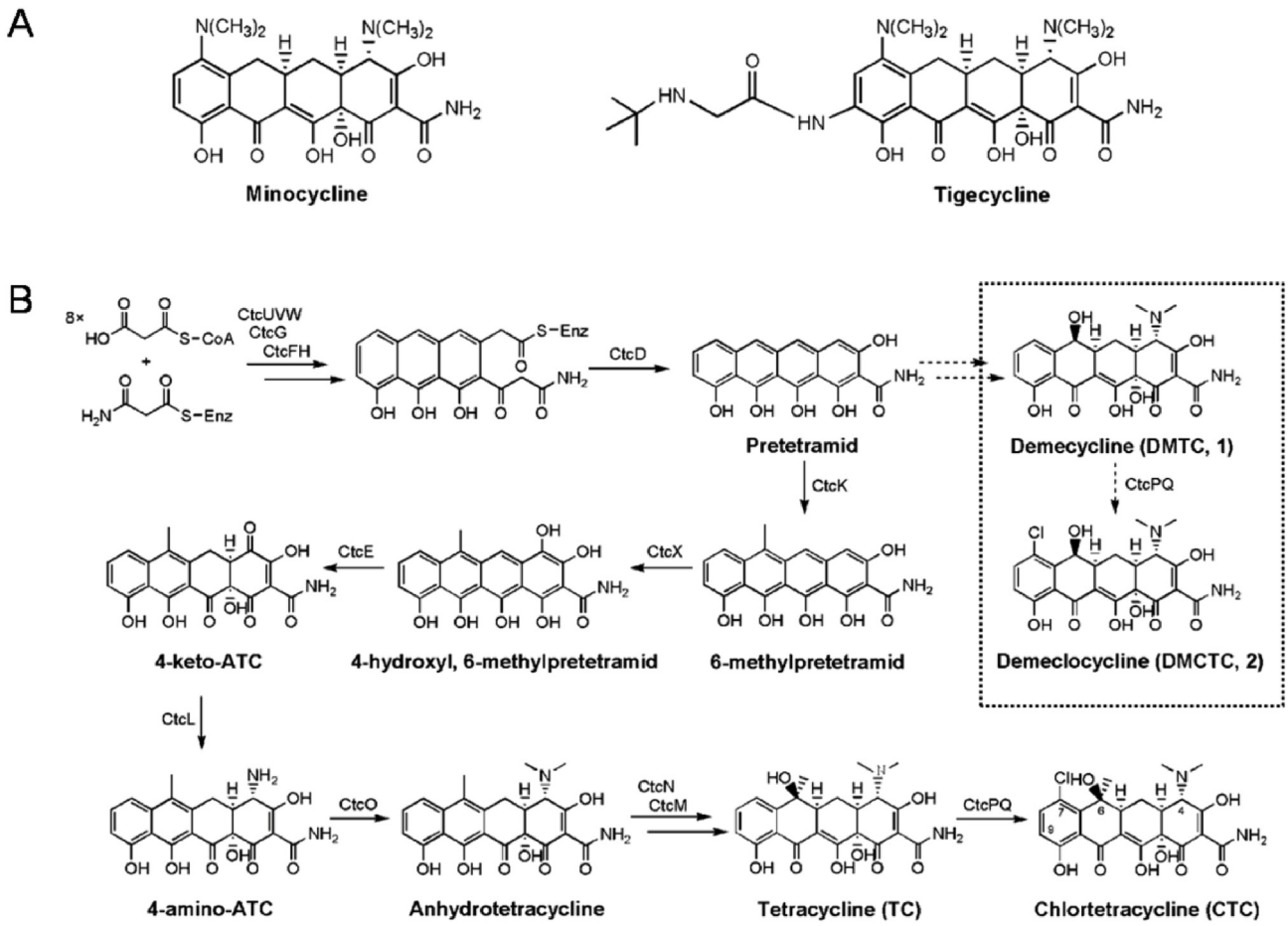

Fig. 1. Representative chemical structures and CTC biosynthetic pathway. (A) Chemical structures of minocycline and tigecycline. (B) The deduced biosynthetic pathway of CTC based on previous studies of OTC. Significant intermediates during the synthetic process are shown. Chemical structures of DMTC and DMTCC accumulated in *ΔctcK* mutant strain are highlighted in the dotted rectangular box.

Table 1
Strains and plasmids used in this study.

Strain or plasmid	Description	Source/Reference
***Streptomyces* strains**		
S. aureofaciens F3	Industrial strain producing CTC	Jinhe biotech. Lt.
ΔctcK	*S. aureofaciens* F3 mutant with a 672 bp fragment of *ctcK* substituted by *aadA* + *oriT* cassette	This study
ΔctcK::*ctcK*	*ctcK* complementary strain	This study
F3::3*ctcP*	ZT09, *ctcP* quadrupled with three extra copies through integrative vector	[35]
3*ctcPΔctcK*	ZT09 mutant with *ctcK* disruption	This study
***E. coli* strains**		
BW25113/pKD46	*E. coli* K-12 derivative: *ΔaraBAD* ΔrhaBAD/*ori*R101 *repA*101 tsP_{araB}^{-} *gam*$^{-}$ *bet*$^{-}$*exo bla*	[37,38]
DH10B	F^{-} *mcrA* Δ(*mrr*$^{-}$*hsdRMS*$^{-}$*mcrBC*)*ϕ80*d *lacZ ΔM15 ΔlacX74 deoR recA1 endA1 ara Δ139 D* (*ara,leu*)*1697 galU galK λ*$^{-}$*rspL nupG*	GibcoBRL
ET12567/pUZ8002	*dam dcm hsdS*/pUZ8002	[47]
BL21Gold (DE3)	F^{-}*ompT hsdS*$_B$($r_B^-m_B^-$) *gal dcm* (DE3) pLysS (Cm^R)	Strategene
Plasmids		
17G4	pCC1FOS derivative with the whole *ctc* gene cluster	[35]
pIJ778	*aadA*, *oriT*	[37,38]
pET28a	Kan^R, pBR322 origin, PT7	Novagen
pJTU968	pRSETb derivative, *bla*, *permE**	[40]
pPM927	*tsr*, *oriT*, *int*, *attP*	[39]
pYWN01	17G4 derivative in which *ctcK* was substituted by *aadA* + *oriT* cassette using PCR-targeting recombination	This study
pYWN02	pET28a derivative with a PCR fragment harboring *ctcK* amplified from *S. aureofaciens* F3 genome and inserted by one-step cloning	This study
pYWN03	pJTU968 derivative with insertion of *Nde*I-*Eco*RI double-digested fragment harboring *ctcK* from pYWN02	This study
pYWN04	pPM927 derivative with insertion of *Mun*I-*Eco*RI double-digested fragment harboring *permE** and *ctcK* from pYWN03	This study

several attempts have been made to produce DMTC and DMCTC by adding certain C-methylation inhibitors to the fermentation broth [28–30], screening for DMTC- and DMCTC-accumulating spontaneous or induced random mutants [31,32], and introducing site specific mutation via DNA recombination to eliminate activity of tentative enzymes responsible for C6-methylation [33,34]. But these methods seemed to be costly and labor-intensive without sufficient understanding of CTC biosynthetic pathway. So, the detailed biosynthetic mechanism of DMTC and DMCTC still await discovery.

In 2013, our group successfully cloned *ctc* gene cluster in the CTC

Table 2
Primers used in this study.

Primer	Sequence (5′-3′)	Use
KTAR-P1	GGCTGACGCCCTGGGCGAGGAGCCGGCCGGCGCGGCCGAATTCCGGGGATCCGTCGACC	Amplification of *aadA* + *oriT* cassette from pIJ778
KTAR-P2	CTGCCGTCCACCAGGTTCTCGACCACGATCACCCGGCTGTGTAGGCTGGAGCTGCTTC	
KYZ-P1	ACGGACGCCTCGGTGTACGTG	Verification of *ΔctcK* mutant strain
KYZ-P2	CATCTGACCCCGCTCCCCTTC	
KEXP-P1	TGCCGCGCGGCAGCCATATGATGACGGACAACGGCGAGATC (*Nde*I site)	Amplification of *ctcK* fragment for insertion into pET28a by one-step cloning
KEXP-P2	TGTCGACGGAGCTCGAATTCTCAGCCCCGTTCGGGCACCAC (*Eco*RI site)	
927YZ-P1	CCCGATGCTAGTCGCGGTTGATC	Verification of *ctcK* complementary strain
927YZ-P2	CGTCGTCCCACTCCAGGATGTTCTT	

high-yielding industrial strain *S. aureofaciens* F3. Based on bioinformatics analysis, genetic manipulation and biochemical characterization of the halogenase CtcP [35], we have proposed a biosynthetic pathway of CTC (Fig. 1B). Pretetramid, the precursor of DMTC and DMCTC, was speculated to be involved in CTC biosynthesis, and the successful transformation of TC to CTC catalyzed by CtcP opened up the possibility that DMCTC might be transformed from DMTC [35,36]. Meanwhile, the structural difference between TC and DMTC, CTC and DMCTC suggested that a methyltransferase might participate in the introduction of C6-methyl. In this study, we demonstrated the function of C-methyltransferase gene *ctcK* in *ctc* cluster. By genetic interruption of *ctcK*, we successfully obtained the DMTC- and DMCTC-producing strain. Moreover, through metabolic engineering optimization of the *ΔctcK* mutant strain, we developed a more productive producer of DMCTC. With further engineering manipulation in future, these two strains reported here could be potential strains providing synthetic precursors for semisynthesis of minocycline, tigecycline and other novel tetracycline derivatives.

2. Materials and methods

2.1. Bacterial strains, plasmids, and general techniques

Strains and plasmids used in this study are listed in Table 1. *S. aureofaciens* F3, the CTC high-yielding industrial strain, was used as the original strain for construction of *ΔctcK* mutant and then the *ctcK* complementary strain. F3:3*ctcP* [35], the *ctcP* overexpression mutant, was used for *ctcK* inactivation to increase CTC yield. *Escherichia coli* BW25113/pKD46, DH10B and ET12567/pUZ8002 were used for gene replacement based on λ-Red-recombination, gene cloning and inter-generic conjugation between *E. coli* and *S. aureofaciens* F3 [37,38], respectively. *E. coli* BL21 Gold (DE3) was used as the host for heterologous protein expression and pET28a was the expression vector. pIJ778 [37,38] was used as the template for amplification of an *aadA* + *oriT* cassette for *ctcK* disruption. pPM927 [39], an integrating vector, was used for *ctcK* complementation and pJTU968 [40] was a transition vector for addition of *permE** before *ctcK* gene. General genetic manipulations of *E. coli* or *Streptomyces* were carried out according to reported procedures [41,42].

S. aureofaciens F3 and its derivative strains were cultured at 30 ˚C on solid YM medium (34% oat flour, 16% agar, 0.005% $MgSO_4$, 0.010% KH_2PO_4 and 0.015% $(NH_4)_2HPO_4$) for sporulation, and SFM medium (2% mannitol, 2% soya flour and 2% agar) was used for conjugation. The seed liquid medium was TSBY (0.5% yeast extract, 3% tryptone soya broth, 10.3% sucrose) and the fermentation medium per liter contained 80.0 g corn starch, 40.0 g soya flour, 1.0 g yeast extract, 14.0 g tryptone, 8.0 g corn milk, 7.0 g $CaCO_3$, 3.5 g $(NH4)_2SO_4$, 2.5 g NaCl, 0.25 g $MgSO_4$ and 15 ml soya bean oil. *E. coli* strains were cultivated at 37 ˚C in LB liquid medium or on LB agar plate.

2.2. Bioinformatics analysis

Homologous proteins of CtcK were identified by online software NCBI Blastp (https://blast.ncbi.nlm.nih.gov/). Multiple sequence alignment was conducted using BioEdit software and the referred homologous proteins were ChdMI (AHD25937.1) from *Amycolatopsis sulphurea*, OxyF (AAZ78330.1) from *Streptomyces rimosus*, DacM1 (AFU65900.1) from *Dactylosporangium* sp. SC14051, BchU (WP_010931722.1) from *Chlorobaculum tepidum* and LaPhzM (AMQ09360.2) from *Lysobacter antibioticus* OH13. The prediction of CtcK's secondary structure was conducted by PredictProtein (https://www.predictprotein.org/) [43] and PSIPRED 4.0 (http://bioinf.cs.ucl.ac.uk/psipred/) [44,45].

2.3. Construction of gene inactivation and complementation mutants

The primers used in this study are listed in Table 2. Fosmid 17G4 was first introduced into *E. coli* BW25113 by electroporation. Plasmid pIJ778 was used as the template for PCR amplification of *aadA* + *oriT* cassette with primers KTAR-P1 and KTAR-P2. Then 672 bp fragment of *ctcK* was replaced by the spectinomycin resistant cassette on 17G4 using PCR-targeting strategy with the help of inducible λ-Red recombinase [37]. After PCR verification and replication in *E. coli* DH10B, the mutant plasmid pYWN01 was finally introduced into *S. aureofaciens* F3 by conjugation between *E. coli* ET12567/pUZ8002 and *Streptomyces*. The potential double-crossover *ΔctcK* strains were firstly obtained from antibiotic selection (spectinomycin 50 μg/ml and nalidixic acid 50 μg/ml) on SFM medium and then incubated on YM medium with the same antibiotics. The positive *ΔctcK* strains were verified by PCR using primers KYZ-P1 and KYZ-P2.

As for *ctcK* complementation, pJTU968-derived plasmid pYWN03 was first constructed by insertion of the complete *ctcK* gene behind *permE** promoter. Then the *permE** + *ctcK* fragment was double-digested from PCR-confirmed pYWN03 by *Mun*I-*Eco*RI and transferred to *Eco*RI-digested integrating vector pPM927. The derivative plasmid pYWN04 was introduced into *ΔctcK* mutant strain by conjugation and positive mutants were firstly selected with spectinomycin and thiostrepton and then verified by PCR using primers 927YZ-P1 and 927YZ-P2.

2.4. Fermentation, isolation and analysis of TCs

Spores stored in 20% glycerol were inoculated in TSBY medium in the proportion of 0.1% and cultivated at 30 ˚C for about 24 h. Then 5 ml seed broth was transferred to 100 ml fermentation medium for another 5 days. As for quantitative fermentation, 1 ml culture was collected and ten times diluted by TSBY medium to monitor its OD_{450}. The transferred volumes were calculated according to it to ensure equal amount of seeds were inoculated in fermentation medium. Proper antibiotics were added in the seed medium when mutant spores were used, and all cultivation procedures were performed in flasks containing coil springs.

After fermentation, pH of the broth was adjusted to 1.5–2.0 with oxalic acid to release products from cells. The lysate mixture was centrifuged and the supernatant was filtrated with 0.22 μm polyether sulfone (PES) membrane. High-performance liquid chromatography (HPLC) was performed on an Agilent HPLC series 1100 system with an Agilent TC-C18 (2) column (5 μm, 4.6 × 250 mm). Separation of

different fermentation products was achieved under a constant flow rate of 0.6 ml/min with 80% buffer A (contained 0.2% formic acid) and 20% buffer B (acetonitrile). All TCs were monitored at 360 nm and DMCTC was quantified on the basis of peak areas from the standard curve established using DMCTC standard. For high-resolution mass measurements, an Agilent 1200 series LC/MSD trap system in tandem with a 6530 Accurate-Mass quadrupole time-of-flight (Q-TOF) mass spectrometer was used with an electrospray ionization source (100–1000 *m/z* mass range, positive mode).

2.5. Time-course analysis of fermentation products in S. aureofaciens mutant

For time-course analysis of fermentation products, 5 ml fermentation broth was removed from the same shake flask every 24 h from Day 2 to Day 5 and stored at 4 ˚C for extraction. Since soya bean oil was added in the fermentation medium, the supernatant of acidified culture broth could not be directly concentrated. Therefore, equal volume of *n*-hexane was used to extract oil out of the broth at room temperature. After extraction of 3–5 times, the remaining broth was freeze-dehydrated in vacuum and the resultant products were dissolved in 100 μl water for HPLC analysis.

2.6. Detection of spontaneous transformation of DMTC and DMCTC

To explore the spontaneous transformation of DMTC and DMCTC, DMTC and DMCTC standards (4*S* configuration) were diluted to 200 μM and 100 μM respectively, which were close to their concentrations in *ΔctcK* fermentation broth. Then 100 μl *ΔctcK* fermentation broth and diluted standards were all half divided and one part was kept at room temperature while the other was stored under −30 ˚C. After 5 days, all samples were analyzed by HPLC.

2.7. Heterologous expression and purification of recombinant CtcK

The complete coding DNA sequence (CDS) flanked by two 20 bp homologous arms was first amplified from the genomic DNA of *S. aureofaciens* F3 using primers KEXP-P1 and KEXP-P2. The two homologous arms respectively carried upstream region including *Nde*I site as well as downstream region including *Eco*RI site of pET28a. Then the specific PCR product was inserted into *Nde*I-*Eco*RI double-digested pET28a plasmid using the Ezmax one-step cloning kit (Tolo Biotech, China), generating recombinant *ctcK* expression vector pYWN02. After confirmation by DNA sequencing, pYWN02 was transformed into *E. coli* BL21Gold (DE3). The resulted transformant was cultured in LB medium containing 50 μg/ml kanamycin at 37 ˚C until OD_{600} reached 0.6, and isopropylthio-β-D-galactoside (IPTG) at a final concentration 0.2 mM was added to induce protein expression. The cells were further cultivated at 30 ˚C for 6 h and harvested by centrifugation (3500 rpm, 15 min, 4 ˚C) and resuspension in 20 ml of buffer A (50 mM Tris-HCl, 300 mM NaCl, pH 8.0).

For purification of the His_6-tagged protein, bacterial cells were lysed by high pressure cracker at 600 bar, then cellular debris was removed by centrifugation (9000 rpm, 1 h). The supernatant filtrated with 0.45 μm PES membrane was loaded on nickel-affinity chromatography to purify CtcK using standard protocols. Eluted with increasing gradient of buffer B (buffer A with 500 mM imidazole), purified protein was concentrated with centrifugal filters (Amicon) and desalted by gel filtration chromatography. Final concentration of the protein was determined with Bradford assay using bull serum albumin (BSA) as a standard, and the protein was stored at −80 ˚C in buffer A with 10% glycerol.

2.8. In vitro enzymatic reactions of CtcK

CtcK was purified to homogeneity. 10 mM DMCTC hydrochloride (USP Reference Standard) was dissolved in water and 10 mM DMTC (CATO Research Chemicals Inc.) was dissolved in 0.1 M hydrochloric acid as stock. Methylation reactions were conducted in the typical 100 μl system previously reported [46] which consisted of 1 mM S-adenosylmethionine (SAM, New England Biolabs Inc.), 1 mM DMTC or DMCTC, and 50 μM methyltransferase CtcK in PBS buffer (10 mM Na_2HPO_4, 1.75 mM KH_2PO_4, 137 mM NaCl, 2.65 mM KCl, pH 7.6). Boiled CtcK was used as negative control and 2 mM $MgSO_4$ was added in the "$+Mg^{2+}$" system to confirm whether it could facilitate methylation reaction. All reactions were started by incubation under 30 ˚C for 12 h. The reactions were quenched by the addition of 100 μl water and 100 μl chloroform. Then the mixtures were vortexed and centrifuged to remove the precipitated protein. The supernatants were vacuum freeze-dehydrated and dissolved in 40 μl water before subjected to HPLC analysis.

3. Results

3.1. The ctc gene cluster encoded a C-methyltransferase CtcK

According to previous bioinformatics analysis, two possible methyltransferases CtcO and CtcK were encoded in the *ctc* gene cluster. CtcO is deduced to be a N-methyltransferase possessing 52% identity with OxyT, which catalyzes a *N, N*-dimethylation reaction to yield anhydrotetracycline (ATC) [48]. CtcK showed 69% sequence identity with the C-methyltransferase OxyF, which is responsible for C-methylation of pretetramid to produce 6-methylpretetramid during OTC biosynthesis [49]. Meanwhile, it exhibited homology with other C-methyltransferases involved in natural product biosynthesis, such as ChdMI (67% identity) from chelocardin-producing strain *Amycolatopsis sulphurea* [50] and DacM1 (66% identity) from dactylocycline-producing strain *Dactylosporangium* sp. SC 14051 [51]. On the other hand, based on the NCBI Blastp analysis, a conserved protein domain corresponding to C20-methyltransferase BchU (identity 23%, PDB code: 1X19) was identified. BchU was reported to methylate cyclic tetrapyrrole chlorin in the bacteriochlorophyll *c* production pathway in photosynthetic green sulfur bacteria *Chlorobaculum tepidum* [52]. To consolidate the finding of CtcK as a C-methyltransferase, the possible secondary structure of it was predicted using PredictProtein and PSIPRED 4.0. The predicted secondary structure possessed a Rossmann-like superfold containing alternating α-helixes and β-strands (Fig. 2), which was similar to LaPhzM (identity 33%, PDB code: 6C5B) from *Lysobacter antibioticus* OH13, an O-methyltransferase participating in myxin biosynthesis [53], and is also a typical feature of Class I methyltransferases [54]. Furthermore, multiple sequence alignment of CtcK and these homologous proteins confirmed the existence of a common glycine-rich SAM-binding motif [54], which was marked by a rectangle in Fig. 2. Taken together, CtcK is probably a SAM-dependent Class I C-methyltransferase.

3.2. ΔctcK strain accumulated DMTC and DMCTC

Based on the bioinformatics analysis of CtcK as a possible C-methyltransferase, it might be responsible for methylation of C6 in CTC biosynthesis. The absence of the methyl group in DMTC and DMCTC might be attributed to the inactivity of CtcK. In order to verify our hypothesis, 672 bp of *ctcK* was replaced by a spectinomycin resistant gene in *S. aureofaciens* F3 genome through homologous recombination (Fig. 3A and B). The *ΔctcK* mutant abolished the production of TC and CTC, but accumulated two new compounds **1** and **2** (Fig. 3C). The retention time and UV absorption spectra of these two compounds were identical with that of DMTC and DMCTC, respectively (Fig. 3C and D). Further Q-TOF mass spectrometry analysis of **1** and **2** gave molecular ion peaks at *m/z* 431.1228 ($[M+H]^+$) and 465.0734 ($[M+H]^+$), which were also consistent with that of DMTC and DMCTC (Fig. 3E). To validate that the production of DMTC and DMCTC were solely due to

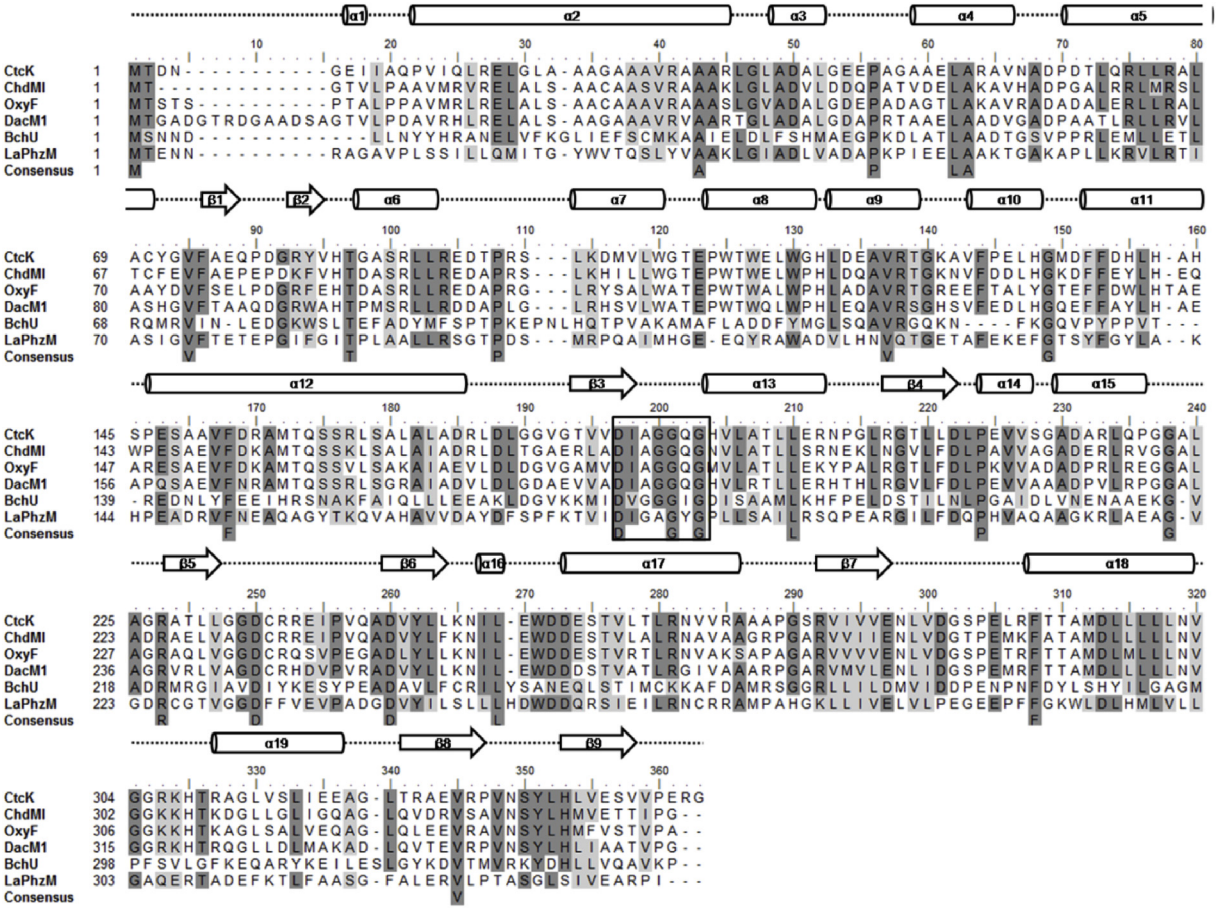

Fig. 2. Sequence alignment of CtcK with other homologous methyltransferases. Residues conserved among them are highlighted in grey. The glycine-rich SAM-binding motif is marked with a rectangular box. The secondary structure was predicted using PredictProtein [43] and PSIPRED 4.0 [44,45]. α-Helixes and β-strands are indicated by cylinders and arrows, respectively.

inactivation of *ctcK*, a copy of *ctcK* on the plasmid pYWN04 under the control of *permE** promoter was introduced into the *ΔctcK* strain. As can be seen in Fig. 3C, the resulted *ctcK* complementary strain recovered TC and CTC production. All results above led to the conclusion that DMTC and DMCTC can be produced by inactivation of the C-methyltransferase gene *ctcK*.

However, based on the previous study of OTC biosynthesis [36], the *ΔctcK* mutant strain should accumulate pretetramid rather than DMTC and DMCTC (Fig. 3). The accumulation of DMTC and DMCTC might result from transformation of intermediates without the C6 methyl by downstream enzymes. To catch pretetramid and any other possible intermediates, we next conducted time-course analysis of the fermentation products in the *ΔctcK* strain by HPLC. 5 ml fermentation broth was sampled from the same shake flask at the same time point from Day 2 to Day 5. Data depicted in Fig. 4A showed that the production of DMTC and DMCTC continuously increased. However, no new product was detected except for two additional peaks with close retention time and identical UV spectra to that of DMTC and DMCTC (Fig. 4A). Inspired by the spontaneous transformation of 4*S*-CTC and 4*S*-TC to their 4*R* epimers at room temperature [35], we wondered whether the two additional peaks were spontaneous transformed DMTC and DMCTC with another configuration. To verify the possibility, DMTC and DMCTC standards (4*S* configuration) as well as unconcentrated sample collected at Day 5 in time-course fermentation process was divided into two equal parts respectively, and each part was kept at room temperature or −30 °C for 5 days. The HPLC profile in Fig. 4B showed that compared to samples kept at −30 °C, 4*S*-DMTC and 4*S*-DMCTC were both reduced at room temperature, but two peaks at 9 min and 13 min obviously rose. These two peaks in *ΔctcK* fermentation sample not only had identical retention time with risen peaks detected in DMTC and DMCTC standards, but also showed *m/z* values corresponding to DMTC and DMCTC in Q-TOF analysis (Fig. 4B). Since DMTC and DMCTC standards have been NMR-characterized by their suppliers to be mixed with a small amount of 4*R* epimers, the above results confirmed that these two peaks were spontaneously transformed 4*R* epimers during the concentration process at room temperature.

The time-course analysis of fermentation products in *ΔctcK* strain did not reveal the accumulation of the proposed substrate of CtcK. Meanwhile, no biosynthetic intermediate for downstream tailoring enzymes has been found. These data suggested that the production of DMTC and DMCTC could be attributed to the relaxed specificity of downstream enzymes. However, the possibility that CtcK might catalyze the direct methylation of DMTC and DMCTC to TC and CTC could not be excluded.

3.3. Heterologous expression and in vitro enzymatic assay of CtcK

Without the pretetramid at hand, we tried testing whether CtcK could catalyze the direct methylation of DMTC and DMCTC. Firstly, the *ctcK* gene was cloned and expressed in *E. coli* BL21Gold (DE3) as a N-His_6 recombinant protein. Then the CtcK protein was purified by nickel-affinity chromatography. The purity and size (39.2 kDa) of the protein were examined by 15% SDS-PAGE (Fig. 5A). Referring to the typical methyltransferase reaction system [46], the reaction was conducted in PBS buffer and SAM was selected as methyl group donor. Unexpectedly, no CTC or TC was generated in the reaction systems even when they

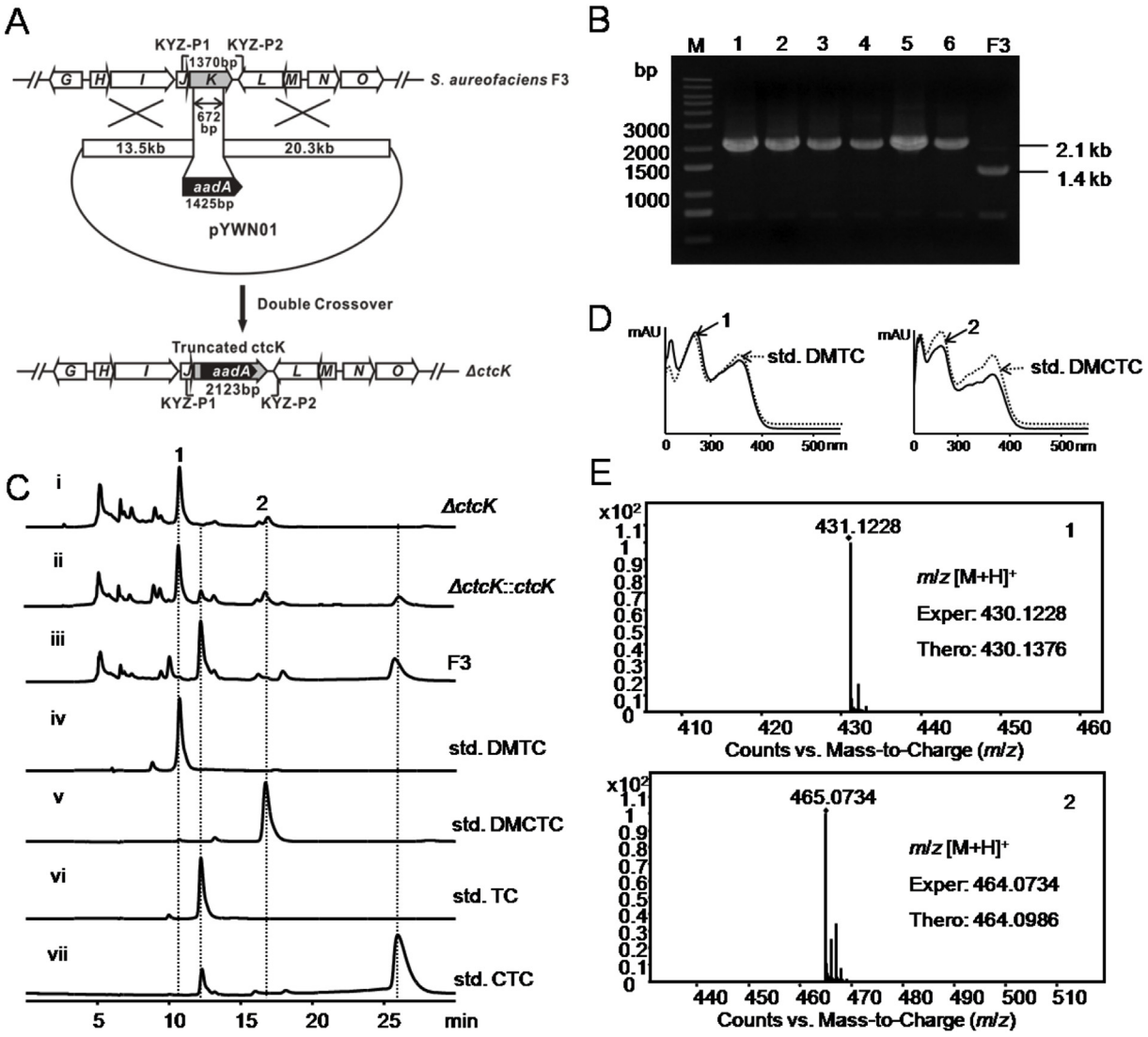

Fig. 3. Construction and fermentation product analysis of the *ΔctcK* mutant strain. (A) The schematic construction of *ctcK* disrupted strain. The 672 bp fragment of *ctcK* was replaced by an *oriT* + *aadA* cassette through fosmid-based homologous recombination. (B) PCR confirmation of *ctcK* gene replacement. Lane 1–6, the *ΔctcK* mutant, in which the mutants give the expected 2.1 kb PCR products. *S. aureofaciens* F3 (F3) produced 1.4 kb products. (C) HPLC profiles of fermentation products of *ΔctcK*, *ΔctcK*:*ctcK* and F3 strains. Compounds **1** and **2** are new products accumulated in *ΔctcK* mutant strain. (D)The UV spectra of compounds **1** and **2** contrasted with DMTC and DMCTC standards respectively. (E) Q-TOF analysis of compounds **1** and **2**.

were incubated overnight at 30 °C (Fig. 5B and C). And addition of $MgSO_4$ led to the occurrence of precipitation, which was possibly because of the chelation between magnesium ion and TCs [55]. It was reported that OxyF, the homologous protein of CtcK, possessed high specificity toward its natural substrates [49], thus the nonreactivity of CtcK on DMTC and DMCTC suggested its strict substrate specificity. In other words, the substrate of CtcK might be an early biosynthetic intermediate involved in CTC biosynthesis.

3.4. Construction of high DMCTC production strain

CtcP is the halogenase that catalyzes the last step, conversion of TC to CTC, in CTC biosynthetic pathway [35]. To enhance its catalytic efficiency, 1–5 copies of *ctcP* was respectively introduced into the F3 strain under the control of constitutive *permE** promoter. Consequently, the integration of three extra copies of *ctcP* (ie, F3:3*ctcP*) could most effectively improve CTC production by 73% in *S. aureofaciens* F3 [35], which implied that the accumulation of DMCTC might also be increased by similar manipulation of *ctcP*. Based on previous studies, we constructed the engineering strain through inactivation of *ctcK* in the F3:3*ctcP* mutant strain (Fig. 6A). As can be seen from Fig. 6B, overexpression of *ctcP* in the *ΔctcK* strain contributed to the increased production of DMCTC. After quantitative analysis, the yield of DMCTC increased 31%, reaching up to 21.6 mg/L. The successful construction of the strain with high DMCTC production set important stage for future yield optimization by metabolic engineering.

4. Discussion

Minocycline and tigecycline (Fig. 1A) are both TCs extensively used in clinical with remarkable potency. Minocycline exhibits a broad antibiotic spectrum including activity against some tetracycline-resistant staphylococci [56], and various non-antibiotic effects of it further extend the field of its application [7]. Tigecycline is referred to as the last line of defense against multidrug-resistant bacteria because it can conquer most of antibiotic resistance mechanisms known in them by virtue of its long glycyl side chain and high binding affinity [56,57]. Currently, a prevalent strategy for production of non-natural tetracycline derivatives is semisynthesis, which means chemical synthesis of final products using natural products as raw materials. As for

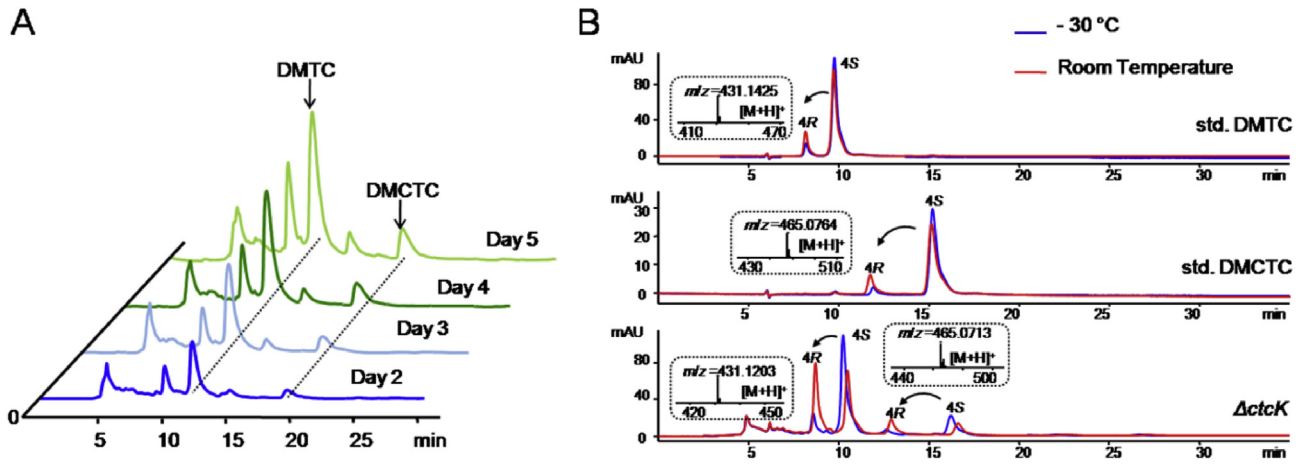

Fig. 4. Time-course fermentation and thermal stability of DMTC and DMCTC. (A) HPLC profiles of time-course fermentation products of *ΔctcK* mutant strain to catch possible intermediates. Samples were removed from the same shake flask every 24 h from Day 2 to Day 5. (B) Spontaneous transformation of 4*S*-DMTC and 4*S*-DMCTC to their 4*R* epimers at room temperature (the red line) in standard DMTC, DMCTC and *ΔctcK* fermentation sample. The same samples stored at −30 °C (the blue line) for the same amount of time (5 days) were also analyzed for comparison. The *m/z* values of spontaneously transformed 4*R* epimers determined by Q-TOF mass spectrometry are shown in the rounded rectangle boxes.

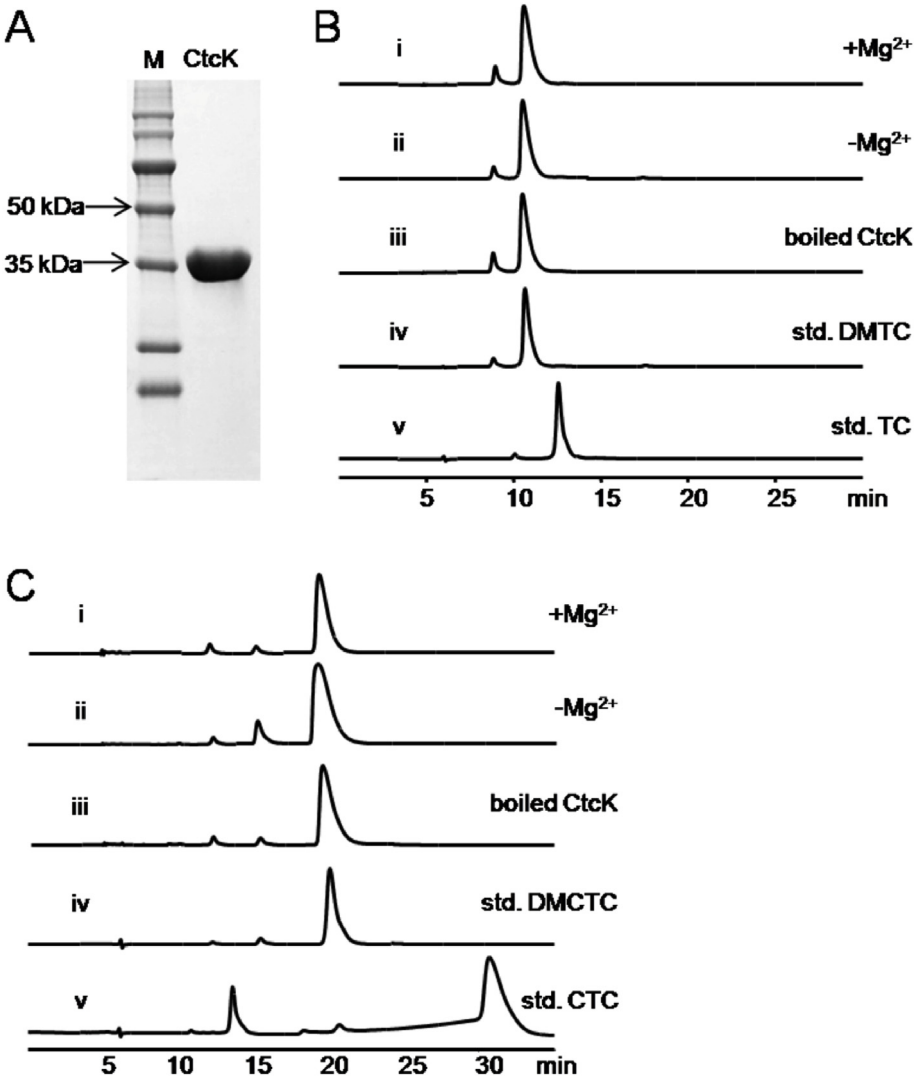

Fig. 5. Characterization of the purified CtcK and its *in vitro* enzymatic assay. (A) SDS-PAGE analysis of the purified His_6-CtcK (M_r = 39.2 kDa). (B) HPLC profiles of CtcK incubated with DMTC in the presence (i) or absence (ii) of Mg^{2+}. The boiled CtcK incubated with DMTC (iii) was used as negative control. iv and v are DMTC and TC standards. (C) HPLC profiles of CtcK incubated with DMCTC in the presence (i) or absence (ii) of Mg^{2+}. The boiled CtcK incubated with DMCTC (iii) was used as negative control. iv and v are DMCTC and CTC standards.

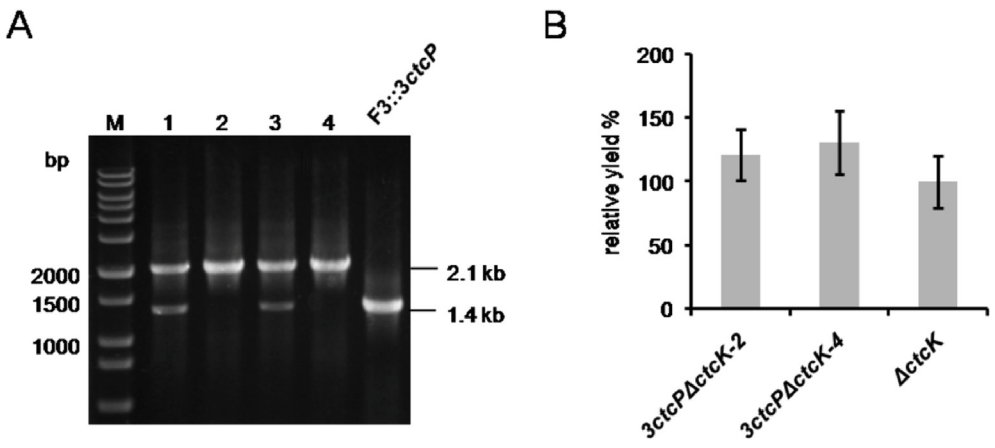

Fig. 6. Construction and DMCTC yield analysis of the 3*ctcP*Δ*ctcK* engineering strain. (A) PCR confirmation of *ctcK* gene replacement in F3:3*ctcP*. Lane 2 and 4, engineering strains with successful *ctcK* disruption. (B) Quantitative analysis of DMCTC yield in strains 3*ctcP*Δ*ctcK*-2, 3*ctcP*Δ*ctcK*-4 and Δ*ctcK*. The productivity of DMCTC in Δ*ctcK* is determined as 1 for comparison and quantitative fermentation was performed in three replicates.

minocycline and tigecycline, their semisynthetic precursors are microbially synthesized DMTC and DMCTC [4,10].

DMTC and DMCTC are C6-demethylated derivatives of TC and CTC, respectively. Both TC and CTC are produced by *S. aureofaciens*, and the biosynthetic studies have been conducted through random mutation and feeding experiments [58]. Induced mutations during this process coincidently generated DMTC- and DMCTC-yielding strains [31,59], but how their genetic and physiological characteristics were varied remained unknown. In order to facilitate directed metabolic engineering of *S. aureofaciens* strains for DMTC and DMCTC production, it is necessary to discuss the biosynthetic mechanism of CTC.

During previous study of CTC in *S. aureofaciens* F3, the complete *ctc* gene cluster has been cloned [35], and the biosynthetic pathway (Fig. 1B) was speculated based on OTC's [36] owing to the high homology of genes involved in these two clusters. Also, the halogenase CtcP was characterized to be responsible for the transformation of TC to CTC by gene inactivation and overexpression. But the function of CtcK was just predicted according to that of its homologous protein OxyF and hasn't been specifically determined.

In this study, we first conducted multiple sequence alignment of CtcK and its homologous proteins, which indicated the conserved SAM-binding motif. Subsequent prediction of its secondary structure revealed typical Rossmann-like superfold of Class I methyltransferases. Disruption of *ctcK* resulted in the accumulation of two new products DMTC and DMCTC, which were confirmed by HPLC and Q-TOF analysis. The absence of 6-methyl suggested the role of CtcK in the methylation of C6. However, the predicted substrate pretetramid of CtcK was not accumulated during the time-course analysis of fermentation products in Δ*ctcK* mutant, while two detected risen peaks were verified by Q-TOF as 4*R*-DMTC and 4*R*-DMCTC resulting from the spontaneous transformation of 4*S*-DMTC and 4*S*-DMCTC, respectively. The production of DMTC and DMCTC in Δ*ctcK* mutant was then attributed to the substrate tolerance of downstream modification enzymes involved in CTC biosynthesis. Consistently, DMTC and DMCTC could not be methylated into TC and CTC in the *in vitro* enzymatic assay of CtcK. This data supported the proposal that CtcK functions at the middle stage of CTC biosynthetic pathway, rather than catalyzes the direct methylation of DMTC and DMCTC into TC and CTC. The attempt to inactivate *ctcK* in overexpression strain of the halogenase CtcP successfully improved DMCTC yield, suggesting the feasibility of rational metabolic engineering to obtain expected products.

However, although overexpression of CtcP in the F3:3*ctcP* mutant strain [35] could drive the transformation of DMTC to DMCTC, a certain amount of DMTC still existed in the fermentation broth probably because of the low halogenation efficiency when the substrate was DMTC rather than TC. As is shown in halogenase engineering studies on tryptophan halogenases RebH and SttH [60–62], structure-based point mutations and directed evolution could broaden the substrate scope thereby improve the reactivity of them [63], which might be practicable ways to provide CtcP with more flexible substrate selectivity. In addition, overexpressing positive regulatory genes or inactivating repressors, increasing intracellular precursor supply and manipulating resistance genes in *ctc* cluster are also potentially useful for DMCTC overproduction to meet commercial needs [64].

On the other hand, the structures of naturally-occurring compounds isolated from the strains lag far behind in terms of structural diversity. Although derivatives with different structural moieties have been isolated by mutating biosynthetic genes, the number and the productivities were limited and this is still the bottleneck of industrial production of new TC derivatives [21,22,31,32]. Fortunately, with the advancement in the field of synthetic biology together with genome sequencing and genome mining techniques, the limitation of biological synthesis could be broken and natural metabolic pathways could be diversified to generate non-natural products possessing novel activities [65,66]. So, it's a more extensive application prospect of DMTC and DMCTC if they can be produced as intermediates in reprogrammed biosynthetic pathways employing heterologous or engineered enzymes to construct more TC derivative antibiotics.

In summary, the detailed functional investigation of the C-methyltransferase CtcK expanded the understanding of CTC biosynthesis. Moreover, an engineering strain that can produce DMTC and DMCTC was successfully conducted by inactivation of *ctcK*. Then yield of DMCTC was improved with the help of three extra copies of the halogenase gene *ctcP*. Compared to random mutation, the direct manipulation of *ctcK* reported here is a more time-saving and convenient way to achieve the biosynthesis of DMTC and DMCTC. Meanwhile, the genetic manipulation of genes within *ctc* cluster doesn't alter the whole genetic background of the strain, which can facilitate subsequent metabolic engineering or other manipulations to construct more productive strains or produce novel TC derivatives.

Funding

This work was supported by grants from National Key R&D Program of China (2018YFA0900400) from the Ministry of Science and Technology; the National Natural Science Foundation of China (31630002, 31770038, 31700029, and 21661140002); Shanghai Pujiang Program from the Shanghai Municipal Council of Science and Technology (12PJD021); and China Postdoctoral Science Foundation (2017M620151).

CRediT authorship contribution statement

Weinan Yang: Investigation, Formal analysis, Writing - original draft. **Lingxin Kong:** Formal analysis, Writing - review & editing. **Qing Wang:** Methodology. **Zixin Deng:** Resources. **Delin You:** Project

administration, Writing - review & editing.

Declaration of competing interest

The authors declare no financial or commercial conflict of interest.

References

[1] Nguyen F, Starosta AL, Arenz S, Sohmen D, Dönhöfer A, Wilson DN. Tetracycline antibiotics and resistance mechanisms. Biol Chem 2014;395(5):559–75.
[2] Brodersen DE, Clemons WM, Carter AP, Morganwarren RJ, Wimberly BT, Ramakrishnan. The structural basis for the action of the antibiotics tetracycline, pactamycin, and hygromycin B on the 30S ribosomal subunit. Cell 2000;103(7):1143–54.
[3] Stephens CR, Beereboom JJ, Rennhard HH, Gordon PN, Murai K, Blackwood RK, et al. 6-deoxytetracyclines. IV. Preparation, C-6 stereochemistry, and reactions. J Am Chem Soc 1963;85(17):2643–52.
[4] Martell MJ, Boothe JH. The 6-deoxytetracyclines. VII. Alkylated aminotetracyclines possessing unique antibacterial activity. J Med Chem 1967;10(1):44–6.
[5] Barza M, Brown RB, Shanks C, Gamble C, Weinstein L. Relation between lipophilicity and pharmacological behavior of minocycline, doxycycline, tetracycline, and oxytetracycline in dogs. Antimicrob Agents Chemother 1975;8(6):713–20.
[6] Klein NC, Cunha BA. Tetracyclines. Med Clin 1995;79(4):789–801.
[7] Garridomesa N, Zarzuelo A, Galvez J. Minocycline: far beyond an antibiotic. Br J Pharmacol 2013;169(2):337–52.
[8] Good M, Hussey D. Minocycline: stain devil? Br J Dermatol 2003;149(2):237–9.
[9] Blum D, Chtarto A, Tenenbaum L, Brotchi J, Levivier M. Clinical potential of minocycline for neurodegenerative disorders. Neurobiol Dis 2004;17(3):359–66.
[10] Sum P, Lee VJ, Testa RT, Hlavka JJ, Ellestad GA, Bloom JD, et al. Glycylcyclines. 1. A new generation of potent antibacterial agents through modification of 9-aminotetracyclines. J Med Chem 1994;37(1):184–8.
[11] Petersen PJ, Jacobus NV, Weiss WJ, Sum P, Testa RT. *In vitro* and *in vivo* antibacterial activities of a novel glycylcycline, the 9-t-butylglycylamido derivative of minocycline (GAR-936). Antimicrob Agents Chemother 1999;43(4):738–44.
[12] Van Ogtrop ML, Andes DR, Stamstad T, Conklin BR, Weiss WA, Craig WA, et al. *In vivo* pharmacodynamic activities of two glycylcyclines (GAR-936 and WAY 152,288) against various gram-positive and gram-negative bacteria. Antimicrob Agents Chemother 2000;44(4):943–9.
[13] Dowzicky MJ, Chmelařova E. Global in vitro activity of tigecycline and linezolid against Gram-positive organisms collected between 2004 and 2009. Int J Antimicrob Agents 2011;37(6):562–6.
[14] Babinchak T, Ellisgrosse EJ, Dartois N, Rose GM, Loh E. The efficacy and safety of tigecycline for the treatment of complicated intra-abdominal infections: analysis of pooled clinical trial data. Clin Infect Dis 2005;41(5):S354–67.
[15] Ellisgrosse EJ, Babinchak T, Dartois N, Rose GM, Loh E. The efficacy and safety of tigecycline in the treatment of skin and skin-structure infections: results of 2 double-blind phase 3 comparison studies with vancomycin-aztreonam. Clin Infect Dis 2005;41(5):S341–53.
[16] Nelson ML, Levy SB. The history of the tetracyclines. Ann N Y Acad Sci 2011;1241(1):17–32.
[17] Zakeri B, Wright GD. Chemical biology of tetracycline antibiotics. Biochem Cell Biol 2008;86(2):124–36.
[18] Duggar BM. Aureomycin: a product of the continuing search for new antibiotics. Ann N Y Acad Sci 1948;1241(1):163–9.
[19] Backus EJ, Duggar BM, Campbell TH. Variation in *Streptomyces aureofaciens*. Ann N Y Acad Sci 1954;60(1):86–95.
[20] Finlay AC, Hobby GL, Pan SY, Regna PP, Routien JB, Seeley DB, et al. Terramycin, a new antibiotic. Science 1950;111(2874):85.
[21] Rhodes PM, Winskill N, Friend EJ, Warren M. Biochemical and genetic characterization of *Streptomyces rimosus* mutants impaired in oxytetracycline biosynthesis. Microbiology 1981;124(2):329–38.
[22] Al-Jawadi M, Calam C. Physiology of a wild strain and high yielding mutants of *Streptomyces rimosus* producing oxytetracycline. Folia Microbiol 1987;32(5):388–401.
[23] Yu L, Cao N, Wang L, Xiao C, Guo M, Chu J, et al. Oxytetracycline biosynthesis improvement in *Streptomyces rimosus* following duplication of minimal PKS genes. Enzym Microb Technol 2012;50(6–7):318–24.
[24] Tang Z, Xiao C, Zhuang Y, Chu J, Zhang S, Herron PR, et al. Improved oxytetracycline production in *Streptomyces rimosus* M4018 by metabolic engineering of the G6PDH gene in the pentose phosphate pathway. Enzym Microb Technol 2011;49(1):17–24.
[25] Yu L, Yan X, Wang L, Chu J, Zhuang Y, Zhang S, et al. Molecular cloning and functional characterization of an ATP-binding cassette transporter OtrC from *Streptomyces rimosus*. BMC Biotechnol 2012;12(1):52.
[26] Yin S, Wang W, Wang X, Zhu Y, Jia X, Li S, et al. Identification of a cluster-situated activator of oxytetracycline biosynthesis and manipulation of its expression for improved oxytetracycline production in *Streptomyces rimosus*. Microb Cell Factories 2015;14(1):46.
[27] Kong L, Liu J, Zheng X, Deng Z, You D. CtcS, a MarR family regulator, regulates chlortetracycline biosynthesis. BMC Microbiol 2019;19(1):1–11.
[28] Perlman D, Heuser LJ, Semar JB, Frazier WR, Boska JA. Process for biosynthesis of 7-chloro-6-demethyltetracycline. J Am Chem Soc 1961;83(21):4481.
[29] Neidleman SL, Bienstock E, Bennett RE. Biosynthesis of 7-chloro-6-demethyltetracycline in the presence of aminopterin and ethionine. Biochim Biophys Acta 1963;71:199–201.
[30] Neidleman SL, Albu E, Bienstock E. Biosynthesis of 7-chloro-6-demethyltetracycline in the presence of certain homocysteine derivatives and methoxinine. Biotechnol Bioeng 1963;5(2):87–9.
[31] Daniel MJR, Raymond JE, Oscar SN. inventors; American Cyanamid Co. assignee. 6-demethyltetracyclines and methods for preparing the same. 1959. United States patent 2878289.
[32] Growich Jr. JA, inventor, American Cyanamid Co. assignee. 7-Chloro-6-demethyltetracycline fermentation. 1971. United States patent 3616239.
[33] Ryan MJ, Lotvin JA, Strathy N, Fantini SE. inventors; American Cyanamid Co. assignee. Cloning of the biosynthetic pathway for chlortetracycline and tetracycline formation and cosmids useful therein. 1996. United States patent 5589385.
[34] Ryan MJ, inventor, American Cyanamid Co. assignee. Strain for the production of 6-demethyltetracycline, method for producing the strain and vector for use in the method. United States patent 5965429. 1999.
[35] Zhu T, Cheng X, Liu Y, Deng Z, You D. Deciphering and engineering of the final step halogenase for improved chlortetracycline biosynthesis in industrial *Streptomyces aureofaciens*. Metab Eng 2013;19:69–78.
[36] Pickens LB, Tang Y. Oxytetracycline biosynthesis. J Biol Chem 2010;285(36):27509–15.
[37] Gust B, Challis GL, Fowler K, Kieser T, Chater KF. PCR-targeted *Streptomyces* gene replacement identifies a protein domain needed for biosynthesis of the sesquiterpene soil odor geosmin. Proc Natl Acad Sci U S A 2003;100(4):1541–6.
[38] Datsenko KA, Wanner BL. One-step inactivation of chromosomal genes in *Escherichia coli* K-12 using PCR products. Proc Natl Acad Sci U S A 2000;97(12):6640–5.
[39] Smokvina T, Mazodier P, Boccard F, Thompson CJ, Guérineau M. Construction of a series of pSAM2-based integrative vectors for use in actinomycetes. Gene 1990;94(1):53–9.
[40] Xu H, Zhang Y, Yang J, Mahmud T, Bai L, Deng Z. Alternative epimerization in C7 N-aminocyclitol biosynthesis is catalyzed by ValD, a large protein of the vicinal oxygen chelate superfamily. Chem Biol 2009;16(5):567–76.
[41] Kieser T, Bibb MJ, Buttner MJ, Chater KF, Hopwood DA. Practical *Streptomyces* genetics vol. 291. Norwich, UK: John Innes Foundation; 2000.
[42] Sambrook J, Russel DW. Molecular cloning: a laboratory manual. third ed. NY: Cold Spring Harbor Laboratory Press; 2001. Cold Spring Harbor.
[43] Rost B, Yachdav G, Liu J. The predictprotein server. Nucleic Acids Res 2004;32(suppl_2):W321–6.
[44] Jones DT. Protein secondary structure prediction based on position-specific scoring matrices. J Mol Biol 1999;292(2):195–202.
[45] Buchan DW, Jones DT. The PSIPRED protein analysis workbench: 20 years on. Nucleic Acids Res 2019;47(W1):W402–7.
[46] Kong L, Zhang W, Chooi Y, Wang L, Cao B, Deng Z, et al. A multifunctional monooxygenase XanO4 catalyzes xanthone formation in xantholipin biosynthesis via a cryptic demethoxylation. Chem Biol 2016;23(4):508–16.
[47] Paget MSB, Chamberlin L, Atrih A, Foster SJ, Buttner MJ. Evidence that the extracytoplasmic function sigma factor σE is required for normal cell wall structure in *Streptomyces coelicolor* A3 (2). J Bacteriol 1999;181(1):204–11.
[48] Zhang W, Watanabe K, Cai X, Jung ME, Tang Y, Zhan J. Identifying the minimal enzymes required for anhydrotetracycline biosynthesis. J Am Chem Soc 2008;130(19):6068–9.
[49] Zhang W, Watanabe K, Wang CCC, Tang Y. Investigation of early tailoring reactions in the oxytetracycline biosynthetic pathway. J Biol Chem 2007;282(35):25717–25.
[50] Lukežic T, Lesnik U, Podgorsek A, Horvat J, Polak T, Sala M, et al. Identification of the chelocardin biosynthetic gene cluster from *Amycolatopsis sulphurea*: a platform for producing novel tetracycline antibiotics. Microbiology 2013;159(12):2524–32.
[51] Wang P, Kim W, Pickens LB, Gao X, Tang Y. Heterologous expression and manipulation of three tetracycline biosynthetic pathways. Angew Chem Int Ed 2012;51(44):11136–40.
[52] Wada K, Yamaguchi H, Harada J, Niimi K, Osumi S, Saga Y, et al. Crystal structures of BchU, a methyltransferase involved in bacteriochlorophyll c biosynthesis, and its complex with S-adenosylhomocysteine: implications for reaction mechanism. J Mol Biol 2006;360(4):839–49.
[53] Jiang J, Guiza Beltran D, Schacht A, Wright S, Zhang L, Du L. Functional and structural analysis of phenazine O-methyltransferase LaPhzM from *Lysobacter antibioticus* OH13 and one-pot enzymatic synthesis of the antibiotic myxin. ACS Chem Biol 2018;13(4):1003–12.
[54] Liscombe DK, Louie GV, Noel JP. Architectures, mechanisms and molecular evolution of natural product methyltransferases. Nat Prod Rep 2012;29(10):1238–50.
[55] Berthon G, Brion M, Lambs L. Metal ion–tetracycline interactions in biological fluids. 2. Potentiometric study of magnesium complexes with tetracycline, oxytetracycline, doxycycline, and minocycline, and discussion of their possible influence on the bioavailability of these antibiotics in blood plasma. J Inorg Biochem 1983;19(1):1–18.
[56] Wright PM, Seiple IB, Myers AG. The evolving role of chemical synthesis in antibacterial drug discovery. Angew Chem Int Ed 2014;53(34):8840–69.
[57] Šeputienė V, Povilonis J, Armalytė J, Sužiedėlis K, Pavilonis A, Sužiedėlienė E. Tigecycline–how powerful is it in the fight against antibiotic-resistant bacteria? Medicina (Kaunas) 2010;46(4):240.
[58] McCormick JRD, Jensen ER, Johnson SJ, Sjolander NO. Biosynthesis of the tetracyclines. IX. 4-aminodedimethylaminoanhydrodemethylchlortetracycline from a mutant of *Streptomyces aureofaciens*. J Am Chem Soc 1968;90(8):2201–2.
[59] McCormick JRD, Sjolander NO, Hirsch U, Jensen ER, Doerschuk AP. A new family of antibiotics: the demethyltetracyclines. J Am Chem Soc 1957;79(16):4561–3.
[60] Glenn WS, Nims E, Oconnor SE. Reengineering a tryptophan halogenase to

preferentially chlorinate a direct alkaloid precursor. J Am Chem Soc 2011;133(48):19346–9.
[61] Shepherd SA, Menon BRK, Fisk H, Struck A, Levy C, Leys D, et al. A structure-guided switch in the regioselectivity of a tryptophan halogenase. Chembiochem 2016;17(9):821–4.
[62] Payne JT, Poor CB, Lewis JC. Directed evolution of RebH for site-selective halogenation of large biologically active molecules. Angew Chem 2015;54(14):4226–30.
[63] Fraley AE, Sherman DH. Halogenase engineering and its utility in medicinal chemistry. Bioorg Med Chem Lett 2018;28(11):1992–9.
[64] Tan G-Y, Liu T. Rational synthetic pathway refactoring of natural products biosynthesis in actinobacteria. Metab Eng 2017;39:228–36.
[65] Hossain GS, Nadarajan SP, Zhang L, Ng T, Foo JL, Ling H, et al. Rewriting the metabolic blueprint: advances in pathway diversification in microorganisms. Front Microbiol 2018;9:155.
[66] Palazzotto E, Tong Y, Lee SY, Weber T. Synthetic biology and metabolic engineering of actinomycetes for natural product discovery. Biotechnol Adv 2019;37(6):107366.